



# Humanized UGT2 and CYP3A transchromosomal rats for improved prediction of human drug metabolism

Yasuhiro Kazuki<sup>a,b,1</sup>, Kaoru Kobayashi<sup>c</sup>, Masumi Hirabayashi<sup>d,e</sup>, Satoshi Abe<sup>b</sup>, Naoyo Kajitani<sup>b</sup>, Kanako Kazuki<sup>b</sup>, Shoko Takehara<sup>b</sup>, Masato Takiguchi<sup>a</sup>, Daisuke Satoh<sup>b</sup>, Jiro Kuze<sup>b,f</sup>, Tetsushi Sakuma<sup>g</sup>, Takehito Kaneko<sup>h,i</sup>, Tomoji Mashimo<sup>i,j</sup>, Minoru Osamura<sup>c</sup>, Mari Hashimoto<sup>c</sup>, Riko Wakatsuki<sup>k</sup>, Rika Hirashima<sup>k</sup>, Ryoichi Fujiwara<sup>k</sup>, Tsuneo Deguchi<sup>l</sup>, Atsushi Kurihara<sup>l</sup>, Yasuko Tsukazaki<sup>m</sup>, Naoto Senda<sup>m</sup>, Takashi Yamamoto<sup>g</sup>, Nico Scheer<sup>n</sup>, and Mitsuo Oshimura<sup>b</sup>

<sup>a</sup>Department of Biomedical Science, Institute of Regenerative Medicine and Biofunction, Graduate School of Medical Science, Tottori University, Yonago, 683-8503 Tottori, Japan; <sup>b</sup>Chromosome Engineering Research Center, Tottori University, Yonago, 683-8503 Tottori, Japan; <sup>c</sup>Graduate School of Pharmaceutical Sciences, Chiba University, Chiba, 260-8675 Chiba, Japan; <sup>d</sup>Center for Genetic Analysis of Behavior, National Institute for Physiological Sciences, Okazaki, 444-8787 Aichi, Japan; <sup>e</sup>Department of Physiological Sciences, School of Life Science, SOKENDAI (The Graduate University for Advanced Studies), Okazaki, 444-8787 Aichi, Japan; <sup>f</sup>Quality and Reliability Assurance Division, Taiho Pharmaceutical Co., Ltd., Tokushima, 771-0194 Tokushima, Japan; <sup>g</sup>Department of Mathematical and Life Sciences, Graduate School of Science, Hiroshima University, Higashi-Hiroshima, 739-8526 Hiroshima, Japan; <sup>h</sup>Division of Science and Engineering, Graduate School of Arts and Science, Iwate University, Morioka, 020-8551 Iwate, Japan; <sup>i</sup>Institute of Laboratory Animals, Graduate School of Medicine, Kyoto University, Kyoto, 606-8501 Kyoto, Japan; <sup>j</sup>Institute of Experimental Animal Sciences, Graduate School of Medicine, Osaka University, Suita, 565-0871 Osaka, Japan; <sup>k</sup>School of Pharmacy, Kitasato University, Minato-ku, 108-8641 Tokyo, Japan; <sup>l</sup>Drug Metabolism and Pharmacokinetics Research Laboratories, Daiichi Sankyo Co., Ltd., Shinagawa-ku, 140-8710 Tokyo, Japan; <sup>m</sup>Tsukuba Bioanalytical Laboratory, Shin Nippon Biomedical Laboratories, Ltd., Tsukuba, 305-0047 Ibaraki, Japan; and <sup>n</sup>Department of Chemistry and Biotechnology, FH Aachen University of Applied Sciences, 52428 Jülich, Germany

Edited by Martin M. Matzuk, Baylor College of Medicine, Houston, TX, and approved January 4, 2019 (received for review May 15, 2018)

Although “genomically” humanized animals are invaluable tools for generating human disease models as well as for biomedical research, their development has been mainly restricted to mice via established transgenic-based and embryonic stem cell-based technologies. Since rats are widely used for studying human disease and for drug efficacy and toxicity testing, humanized rat models would be preferred over mice for several applications. However, the development of sophisticated humanized rat models has been hampered by the difficulty of complex genetic manipulations in rats. Additionally, several genes and gene clusters, which are megabase range in size, were difficult to introduce into rats with conventional technologies. As a proof of concept, we herein report the generation of genomically humanized rats expressing key human drug-metabolizing enzymes in the absence of their orthologous rat counterparts via the combination of chromosome transfer using mouse artificial chromosome (MAC) and genome editing technologies. About 1.5 Mb and 700 kb of the entire UDP glucuronosyltransferase family 2 and cytochrome P450 family 3 subfamily A genomic regions, respectively, were successfully introduced via the MACs into rats. The transchromosomal rats were combined with rats carrying deletions of the endogenous orthologous genes, achieved by genome editing. In the “transchromosomal humanized” rat strains, the gene expression, pharmacokinetics, and metabolism observed in humans were well reproduced. Thus, the combination of chromosome transfer and genome editing technologies can be used to generate fully humanized rats for improved prediction of the pharmacokinetics and drug–drug interactions in humans, and for basic research, drug discovery, and development.

humanized animal model | mouse artificial chromosome | chromosome transfer | genome editing | transchromosomal rat

**G**enomically humanized animals obtained by the introduction of entire human genomic loci into model organisms are invaluable tools as disease models, for investigating cis-acting regulatory elements, and understanding their role in domainwide regulation, as well as for several biomedical applications (1). The development of humanized animal models has been mainly limited to mice via transgenic and embryonic stem (ES) cell-based technologies (2). Since rats are widely used animal models for studying human disease and for testing the efficacy and toxicity of drugs, their humanization would be more preferable over that of mice for various applications (3, 4). However, since complex manipulation in rat ES cells is much more challenging,

megabase (Mb)-sized humanized rat models have yet to be developed, possibly owing to the chromosomal instability during long in vitro culture (5).

The generation of humanized mouse models with Mb-sized human genomic loci is very difficult via conventional gene transfer techniques, including the use of plasmids, P1-derived artificial chromosomes (PACs), and bacterial artificial chromosomes (BACs), due to the capacity for cloning DNA (6–8). To overcome this obstacle, sequential recombinase-mediated cassette exchange (S-RMCE) or sequential knockin via BACs in mouse ES cells was used to develop humanized mice with Mb-sized large genomic DNA (9, 10). However, these methods are very laborious owing to the requirement for more than five

## Significance

Genomically humanized animals overcoming species differences are invaluable for biomedical research. Although rats would be preferred over mice for several applications, generation of a humanized model is restricted to mice due to the difficulty of complex genetic manipulations in rats. In this study, we successfully generated humanized rats with megabase-sized gene clusters via combination of chromosome transfer using mouse artificial chromosome vector and genome editing technologies. In the humanized UGT2 and CYP3A transchromosomal rats described in this paper, the expression of the human genes, as well as the pharmacokinetics and metabolism of relevant probe substrates, accurately mimic the situation in humans. Thus, the advanced technologies can be used to generate fully humanized rats useful for biomedical research.

Author contributions: Y.K., K. Kobayashi, T.S., T.M., and R.F. designed research; Y.K., K. Kobayashi, M. Hirabayashi, S.A., N.K., K. Kazuki, S.T., M.T., D.S., J.K., T.S., T.K., T.M., M. Osamura, M. Hashimoto, R.W., R.H., R.F., T.D., A.K., Y.T., N. Senda, T.Y., and M. Oshimura performed research; T.S. and T.Y. contributed new reagents/analytic tools; Y.K., K. Kobayashi, S.A., K. Kazuki, S.T., J.K., R.F., T.D., A.K., Y.T., N. Senda, N. Scheer, and M. Oshimura analyzed data; Y.K., K. Kobayashi, S.A., R.F., N. Scheer, and M. Oshimura wrote the paper; and Y.K., K. Kobayashi, T.Y., N. Scheer, and M. Oshimura supervised the study.

The authors declare no conflict of interest.

This article is a PNAS Direct Submission.

This open access article is distributed under [Creative Commons Attribution-NonCommercial-NoDerivatives License 4.0 \(CC BY-NC-ND\)](https://creativecommons.org/licenses/by-nc-nd/4.0/).

<sup>1</sup>To whom correspondence should be addressed. Email: [kazuki@grape.med.tottori-u.ac.jp](mailto:kazuki@grape.med.tottori-u.ac.jp).

This article contains supporting information online at [www.pnas.org/lookup/suppl/doi:10.1073/pnas.1808255116/-DCSupplemental](http://www.pnas.org/lookup/suppl/doi:10.1073/pnas.1808255116/-DCSupplemental).

Published online February 4, 2019.

rounds of cloning, selection of correctly targeted mouse ES cell clones, and testing their capacity to form chimeric mice at each step.

This challenge was addressed by applying transchromosomal (Tc) technology using human chromosome fragments (hCFs), or human artificial chromosomes (HACs), to generate mice with Mb-sized segments of the human genome (11–17). The most significant problem with freely segregating chromosomes with human centromeres has been mosaicism, possibly owing to the instability of hCFs or HACs in mice. Thus, to improve the stability, we constructed mouse artificial chromosome (MAC) vectors from a native mouse chromosome by chromosome engineering (18). The MAC vector was more stable in adult tissues and hematopoietic cells in mice than hCFs or HAC vectors (18, 19). However, the cloning of large Mb-sized segments from human chromosomes into MACs and the application of Tc technology with hCFs/HACs/MACs to rats have not been reported.

Since the Tc technology can introduce a Mb-sized human gene but not disrupt the orthologous gene, the Tc technologies are required to combine with knockout (KO) technologies such as conventional KO technologies in mouse ES cells or genome editing to generate fully humanized animal models. Genome editing technologies, such as zinc-finger nuclease (ZFN), transcription activator-like effector nuclease (TALEN), and clustered regularly interspaced short palindromic repeats/CRISPR-associated protein 9 (CRISPR/Cas9), were utilized to induce mutations or large genomic deletions for orthologous gene cluster KO animals (20–24).

In the present study, we established a strategy for the development of Mb-sized gene cluster humanized rat models by combining MAC-mediated genomic transfer (MMGT) and genome editing technologies. As a proof of concept, we targeted the UDP glucuronosyltransferase family 2 (UGT2) gene cluster and the cytochrome P450 family 3 subfamily A (CYP3A) gene cluster because of their important roles in drug metabolism and the reported species differences in these genes between humans and rodents (25, 26). Although the UDP glucuronosyltransferase family 1 (UGT1) has a very important role in drug metabolism (27), we decided to select the comparably important UGT2 cluster for humanization because of its significantly larger size (~1.5 Mb versus ~200 kb), allowing for more challenging validation of the technology. We established stable humanized Tc rat lines harboring a ~1.5-Mb region including the *UGT2* cluster (10 coding genes) from human chromosome 4 (hChr.4) or a ~700-kb region including the *CYP3A* cluster (four coding genes) from hChr.7 by the transfer of MACs with desired gene clusters. Furthermore, we disrupted the endogenous rat *Ugt2* gene cluster (~762 kb) or rat *Cyp3a* (*Cyp3a23/1* and *Cyp3a2*) using genome editing technologies. We also confirmed the retention of the MAC, and the expected tissue-specific expression and enzymatic function of the UGT2 and CYP3A enzymes in rats.

## Results

**Construction of UGT2-MAC and CYP3A-MAC.** A MAC vector stably maintained in mice has been developed and various small- to intermediate-size genes of interest from circular vectors such as plasmids, PACs, and BACs have been transferred to the MAC vector by a site-specific recombination system for several applications (28–30). However, the loading of a large Mb-sized gene cluster to the MAC vectors has not been demonstrated yet. In this study, the HAC-mediated Mb-sized gene cloning system developed previously was thus applied to the MAC vector and the MMGT was applied to rat (31, 32). To generate “humanized” Tc rats with the entire human *UGT2* cluster (10 coding genes: *UGT2B4*, *UGT2B7*, *UGT2B10*, *UGT2B11*, *UGT2B15*, *UGT2B17*, *UGT2B28*, *UGT2A1*, *UGT2A2*, and *UGT2A3*) or *CYP3A* cluster (4 coding genes: *CYP3A4*, *CYP3A5*, *CYP3A7*, and *CYP3A43*), two MACs containing these clusters were con-

structed using the Cre/loxP-mediated Mb-sized gene cloning system (Fig. 1).

To clone ~1.5 Mb of the *UGT2* cluster on hChr.4 into a MAC (MAC4), hChr.4 was transferred from mouse A9 cells to homologous recombination-proficient DT40 cells using microcell-mediated chromosome transfer (MMCT). The hChr.4 was truncated at the AC125239 locus and a loxP sequence was introduced into the AC074378 locus on the hChr.4 in DT40 cells (Fig. 2A and *SI Appendix*, Figs. S1–S3). The modified hChr.4, hChr.4- $\Delta$ AC125239-loxP in DT40 cells was then introduced into Chinese hamster ovary (CHO) cells containing one of the MAC vectors (MAC4 with hygromycin resistant gene, EGFP gene, and loxP) using MMCT to obtain hybrid CHO clones with two different exogenous chromosomes: the MAC4 and the modified hChr.4 (hChr.4- $\Delta$ AC125239-loxP). To induce reciprocal translocation between the MAC4 and the modified hChr.4, Cre expression vectors were transfected into the CHO hybrids, and recombinant clones were selected. Two out of six drug-resistant clones were PCR positive with *UGT2* cluster-, MAC-, and HPRT-reconstitution-specific primers (*SI Appendix*, Fig. S4). Fluorescence in situ hybridization (FISH) analyses showed that the defined region of hChr.4 containing the *UGT2* cluster had been cloned into the MAC4 vector in the CHO hybrid cells (designated UGT2-MAC) (Fig. 2A). The CYP3A-MAC was also constructed as described above for the UGT2-MAC (Fig. 2B and *SI Appendix*, Figs. S5–S7).

**Generation of Tc Mice with CYP3A-MAC.** Before the generation of Tc rats with the MACs, the MAC function was tested in mice because no MAC with a Mb-sized gene or gene cluster had ever been transferred in mice. Tc mice with the CYP3A-MAC and fully humanized CYP3A (CYP3A-MAC/Cyp3a-KO) mice were generated. FISH, flow cytometry (FCM), reverse transcription-PCR (RT-PCR), and drug-metabolizing activity analyses showed that the CYP3A-MAC was functional and more stably maintained than CYP3A-HAC in mice, and that the CYP3A-MAC has the same stability as the empty MAC (*SI Appendix*, Figs. S8–S11) (16, 18).

**Generation of Tc Rats with UGT2-MAC or CYP3A-MAC.** Establishment of germline-competent rat ES cells with the MAC-carrying gene cluster is challenging due to chromosome instability of rat ES cells during long-term culture. The UGT2-MAC and CYP3A-MAC were introduced into a male rat ES cell line (BLK2i-1) via CHO cells using MMCT. PCR analyses using primers for the detection of the UGT2-MAC or CYP3A-MAC showed that 12 of 22 BLK2i-1 (UGT2-MAC) clones and 11 of 12 BLK2i-1 (CYP3A-MAC) clones contained intact UGT2-MAC and CYP3A-MAC, respectively. FISH analyses showed that the UGT2-MAC and the CYP3A-MAC were present as an individual chromosome without integration into the host rat chromosomes in BLK2i-1 (UGT2-MAC) and BLK2i-1 (CYP3A-MAC) clones, respectively (Fig. 2C and F). Two BLK2i-1 (UGT2-MAC) clones and 4 BLK2i-1 (CYP3A-MAC) clones that were karyotypically normal were used for the subsequent production of chimeras.

In the case of UGT2-MAC rat chimera production, among 13 male chimeric rats, 2 (15%) were capable of germline transmission (Fig. 2D and Table 1). FISH analyses showed that a single UGT2-MAC was contained in the Tc rat (Fig. 2E). In the case of CYP3A-MAC rat chimera production, among 31 male chimeric rats, 11 (35%) were capable of germline transmission (Fig. 2G and Table 1). FISH analyses showed that a single CYP3A-MAC was contained in the Tc rat (Fig. 2H). Taken together, the MACs with gene cluster were successfully transferred to germline-competent rat ES cells and transmitted through the germline. The germline-transmitted Tc UGT2-MAC rats and Tc CYP3A-MAC rats were mated with the *Ugt2*-KO rats and *Cyp3a*-KO rats, respectively, to generate humanized rats, as described below. Both humanized UGT2 and

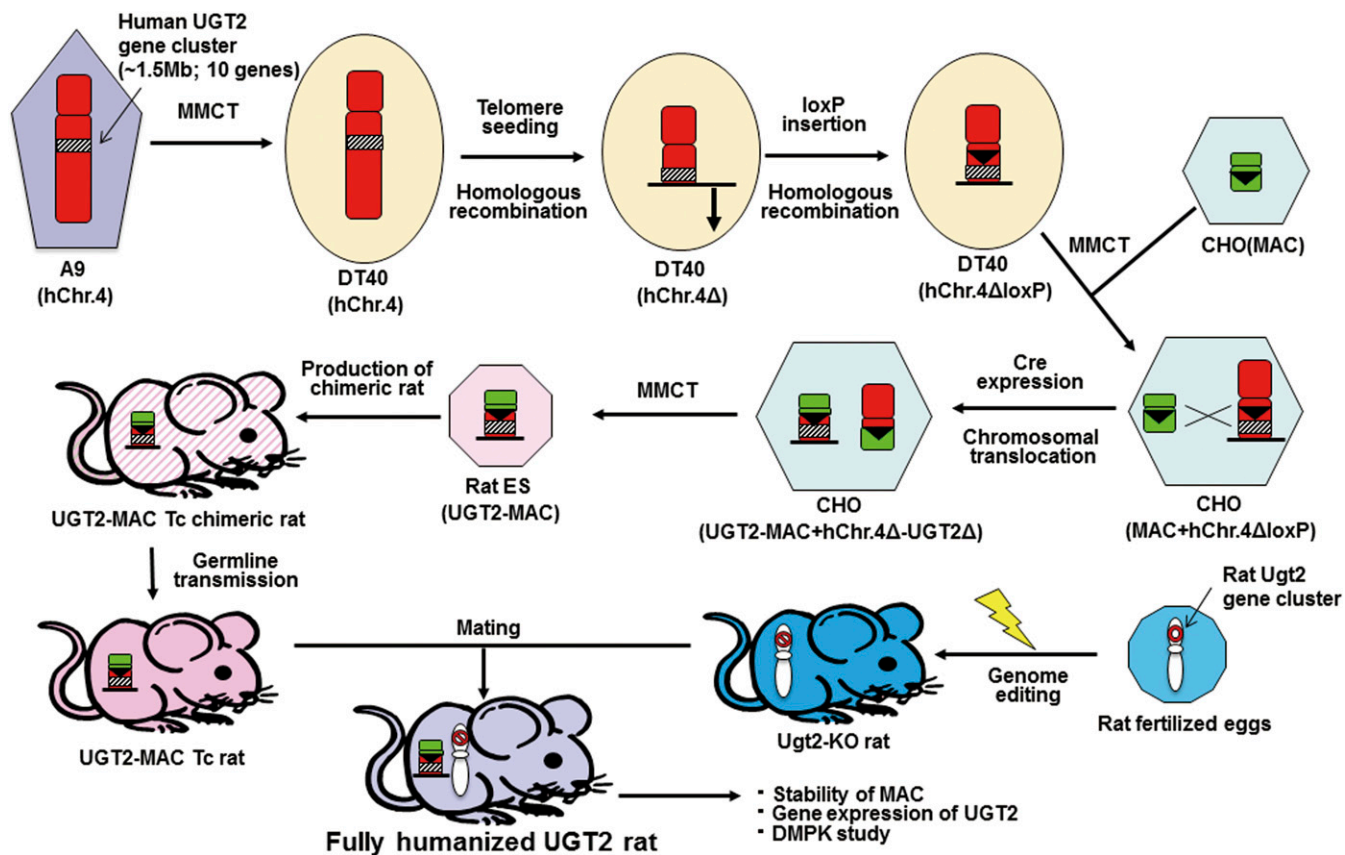


**Fig. 1.** Construction of UGT2-MAC and production of fully humanized UGT2 rats. A schematic diagram of UGT2-MAC construction and fully humanized UGT2 rat production. hChr.4 was transferred from A9 cells to DT40 cells via MMCT and modified in DT40 cells. Telomere-associated chromosomal truncation was carried out at the telomere side of the UGT2 cluster and loxP insertion was conducted at its centromere side in DT40 cells. Modified hChr.4 was transferred to CHO cells containing the MAC vector via MMCT. Cre/loxP-mediated reciprocal translocation generated the UGT2-MAC and a by-product. The UGT2-MAC was transferred to rat ES cells and chimeric Tc rats were produced. Tc rat lines generated through germline transmission were further mated with KO rats generated by genome editing to produce fully humanized UGT2 rats.

CYP3A rats transmitted the UGT2-MAC and CYP3A-MAC, respectively, stably at least beyond the F<sub>8</sub> generation.

#### Generation of Ugt2-KO and Cyp3a-KO Rats.

**Ugt2 cluster KO.** The simultaneous formation of two double-strand breaks (DSBs) causes the joining of separate breakage sites, resulting in loss of the region between the two DSB sites. Only *Ugt2* genes are included in the rat *Ugt2* cluster, which allowed us to apply the large deletion approach for the generation of Ugt2 KO rats. To produce *Ugt2* cluster (~762-kb) KO rats, we simultaneously induced two targeted DSBs in the rat genome using the CRISPR/Cas9 system. hCas9 mRNA and two gRNAs with target sites upstream of *Ugt2a1* and the coding region of *Ugt2b31*-like were injected into rat fertilized eggs (Fig. 3A). Finally, we obtained one *Ugt2* cluster KO rat strain with concatenation of the genomic sequence upstream of *Ugt2a1*, a 102-bp insertion, and the *Ugt2b31*-like region. To confirm the disruption of rat UGT2 function, gemfibrozil glucuronidation activity, a typical marker activity of UGT2 enzymes, was then investigated in the F<sub>2</sub> rats with homozygous deletion (33). The gemfibrozil glucuronidation activity test revealed the decrease of metabolic activity in the liver of Ugt2-KO rats compared with that of wild-type (WT) rats (Fig. 3B). These results suggested the functional deletion of rat *Ugt2* genes in the Ugt2-KO rats. The Ugt2 cluster KO rats were mated with the Tc UGT2-MAC rats to generate fully humanized UGT2 rats (designated UGT2-MAC/Ugt2-KO rats). The Ugt2-KO and UGT2-MAC/Ugt2-KO rats did not display any obvious physiological abnormalities. They grew up without any

significant abnormalities, especially in terms of body weight, and showed no anatomical differences compared with the WT controls. **Cyp3a-KO.** Among rat Cyp3as, *Cyp3a23/3a1* and *Cyp3a2* are the major CYP3A enzymes in the liver (34, 35). In addition, these enzymes can metabolize some prototypical substrates of human CYP3A enzymes (36, 37). Thus, in this study, we decided to disrupt the most important Cyp3a genes, *3a23/3a1* and *3a2*, via TALEN. A pair of TALEN mRNAs targeting exon 5 of rat *Cyp3a23/3a1* and *Cyp3a2* were injected into rat fertilized eggs (Fig. 3C and *SI Appendix*, Fig. S12). Finally, we produced two independent homozygous big deletion (BD) mutants (derived from nos. 32 and 58) and four independent homozygous insertion/deletion mutants including the 3-bp insertion (derived from no. 51), the 1-bp deletion (derived from no. 62), the 9-bp deletion, and the 30-bp deletion (each derived from no. 65). To confirm the disruption of rat CYP3A function, the metabolic activity of triazolam, a typical marker of the activity of CYP3A enzymes (38), was then investigated in the six homozygous rat lines. Triazolam metabolic activity testing revealed the loss of CYP3A activity compared with that of WT rats and humans in five out of the six lines, but not in one line (no. 62) (Fig. 3D). We randomly selected two lines, no. 65 with the 9-bp deletion (designated #65del9) and no. 58 with a BD mutation (designated #58) for further investigation. As with rat *Cyp3a2* BD for #65del9 and #58 (*SI Appendix*, Fig. S12B), rat Cyp3a was considered to be functionally deleted in both lines by disruption of *Cyp3a23/3a1* and *Cyp3a2* via TALEN (Cyp3a-KO). Thus, the #58- and #65del9-Cyp3a-KO rat strains were selected for the production

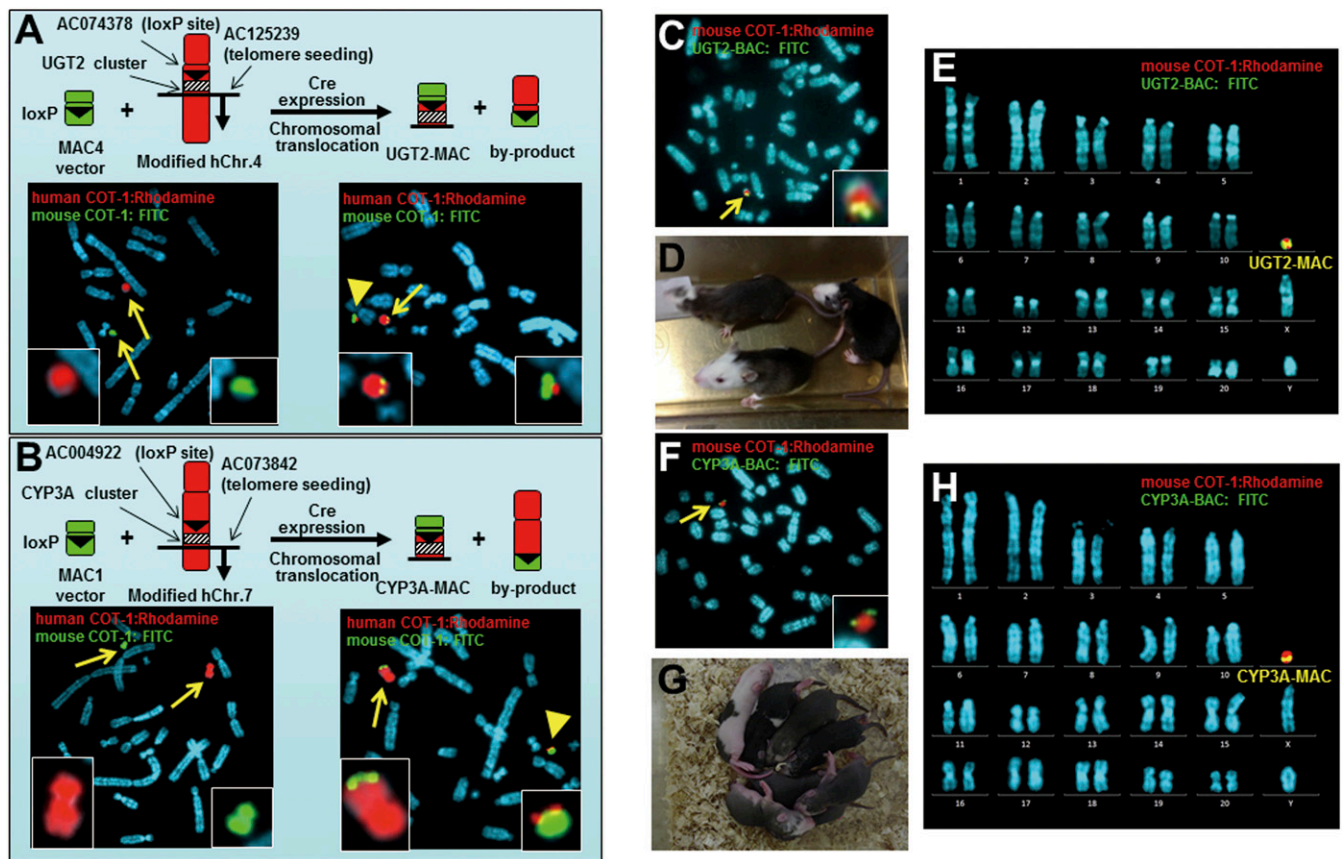


**Fig. 2.** Construction of UGT2-MAC and CYP3A-MAC, and production of Tc rats carrying UGT2-MAC or CYP3A-MAC. (A) Process of UGT2-MAC construction. hChr.4 was truncated at the AC125239 locus and loxP was inserted at the AC074378 locus. The UGT2 cluster was cloned into the MAC4 via a Cre/loxP-mediated reciprocal translocation cloning system. Lower shows FISH images before and after translocation cloning in CHO cells. Left shows CHO cells containing the modified hChr.4 and the MAC4. Right shows CHO cells containing the UGT2-MAC and by-product. The arrowhead indicates the UGT2-MAC. (B) Process of CYP3A-MAC construction. hChr.7 was truncated at the AC073842 locus and a loxP site was inserted at the AC004922 locus. The CYP3A cluster was cloned into the MAC1 as described for the UGT2-MAC construction. Lower shows FISH images before and after translocation cloning in CHO cells. Left shows CHO cells containing the modified hChr.7 and the MAC1. Right shows CHO cells containing the CYP3A-MAC and by-product. The arrowhead indicates the CYP3A-MAC. (C) FISH image of rat ES cell containing the UGT2-MAC. The arrow shows the UGT2-MAC and the *Inset* presents an enlarged image of it. (D) Chimeric rats obtained via injection of rat ES cells carrying the UGT2-MAC. (E) Karyotype of Tc rat containing the UGT2-MAC. (F) FISH image of rat ES cell containing the CYP3A-MAC. The arrow shows the CYP3A-MAC and the *Inset* presents an enlarged image of it. (G) Chimeric rats obtained via injection of rat ES cells carrying the CYP3A-MAC. (H) Karyotype of Tc rat containing the CYP3A-MAC.

of humanized CYP3A rats. The *Cyp3a*-KO rats were mated with the Tc CYP3A-MAC rats to generate CYP3A-humanized rats (designated CYP3A-MAC/*Cyp3a*-KO rats). As in the *Ugt2*-KO and UGT2-MAC/*Ugt2*-KO rats, the resultant *Cyp3a*-KO and CYP3A-MAC/*Cyp3a*-KO rats also did not display any obvious physiological or anatomical abnormalities.

**Characterization of UGT2- and CYP3A-Humanized Rats.** EGFP encoded by the UGT2-MAC/CYP3A-MAC was expressed in all tis-

sues examined, suggesting that the UGT2-MAC/CYP3A-MAC was retained in the respective organs (Fig. 4 A and E). FISH analyses showed that the UGT2-MAC and CYP3A-MAC was detected in  $\geq 84\%$  and  $\geq 90\%$  of cells, respectively, in all examined tissues, including the liver, intestine, kidney, spleen, lung, heart, muscle, thymus, brain, and testis (Fig. 4 B, C, F, and G). To confirm expression of the genes from the UGT2-MAC/CYP3A-MAC, RT-PCR analyses were conducted on various tissues from the Tc rat. In the UGT2-MAC/*Ugt2*-KO rats, *UGT2A3* was expressed in

**Table 1.** Production of chimeric Tc rat and germline-transmitted Tc rat

Gene	Line no.	No. of injected embryos	No. of embryos developed to pups (%)	No. of pups analyzed	No. of chimeras (%)	GT chimeras/total
						male chimeras
UGT2	1	33	13 (39)	13	10 (77)	2/8
	2	60	36 (60)	35	19 (54)	0/5
CYP3A	4	35	11 (31)	11	9 (82)	4/7
	8	60	21 (35)	21	18 (86)	4/8
	11	70	46 (66)	46	30 (65)	2/9
	21	36	22 (61)	22	21 (95)	1/7

GT, germline transmission.

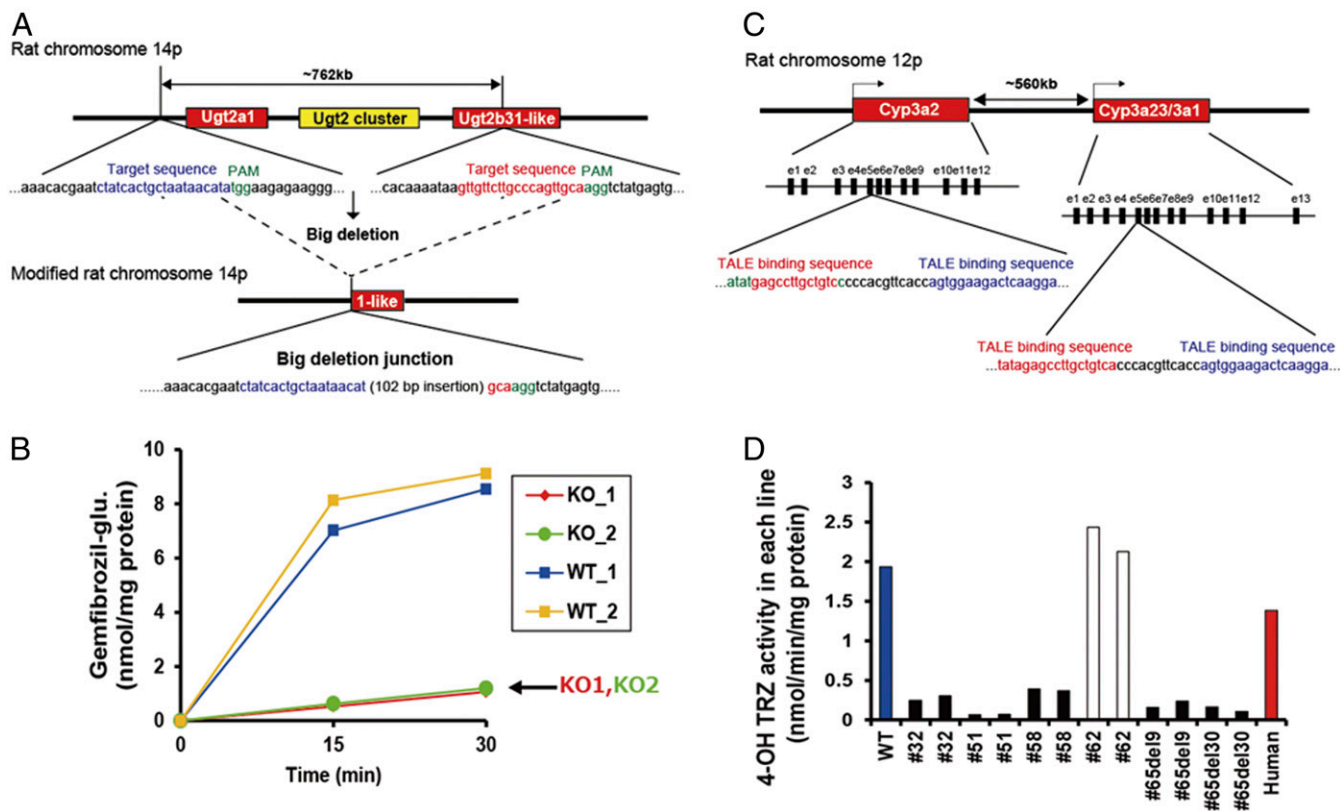


**Fig. 3.** Production of Ugt2 cluster KO, and Cyp3a23/3a1 and Cyp3a2 KO rats, and enzyme activities in their liver microsomes. (A) Schematic view of the rat Ugt2 cluster genomic region and the CRISPR/Cas9-induced large deletion. Blue and red represent the target sequences of each gRNA. Protospacer adjacent motif (PAM) sequences are highlighted in green. The junction sequence after deletion of the Ugt2 cluster is shown at the *Bottom*. (B) Gemfibrozil was time-dependently incubated with liver microsomes prepared from WT and Ugt2-KO rats. The concentration of gemfibrozil glucuronide is shown. (C) Schematic view of the rat Cyp3a23/3a1 and Cyp3a2 genomic region and sites of gene disruption by TALEN. Exon/intron structures are shown. *Left* and *Right* TALEN target sequences are highlighted in red and blue, respectively. Mismatches are shown in green. (D) Results of 4-OH triazolam activity for each strain ( $n = 2$ ). Liver microsomes were incubated with 200  $\mu$ M triazolam for 30 min. Formation of 4-OH triazolam was determined using HPLC. Data are the mean of duplicate assays.

the liver, small intestine, and kidney; *UGT2B4* was mainly expressed in the liver; *UGT2B7* was expressed in the liver, small intestine, kidney, and lung; *UGT2B10* was expressed in the liver; *UGT2B11* was mainly expressed in the liver, small intestine, and kidney; *UGT2B15* was mainly expressed in the liver, small intestine, lung, brain, and testis; and *UGT2B28* was mainly expressed in the liver, small intestine, and kidney (Fig. 4D). These expression profiles are largely consistent with those observed in humans (39). To confirm the effect of UGT2 KO and humanization on the expression of the related endogenous Ugt1 drug-metabolizing enzymes, we determined the relative expression levels of rat *Ugt1a1*, *Ugt1a5*, and *Ugt1a8* in the liver of WT, Ugt2-KO, and UGT2-MAC/Ugt2-KO rats. We selected those genes because a previous report showed that their hepatic expression levels in WT rats were remarkably high compared with those in other tissues (40). According to our results, there was no significant difference in the hepatic expression levels of these genes among the three different rat lines (SI Appendix, Fig. S13). Therefore, Ugt2 KO and humanization do not significantly affect the expression of the endogenous rat Ugt1 genes that we analyzed in this study.

In the CYP3A-MAC/Cyp3a-KO rats, both *CYP3A4* and *CYP3A5* were robustly expressed in the liver and small intestine, and *CYP3A5* additionally in the lung (Fig. 4H). This expression profile is consistent with the one observed in the previously generated humanized CYP3A-HAC mice and in humans (16, 41, 42). To confirm the effect of Cyp3a KO and humanization on the expression of other major Cyp enzymes in rat livers (43), we determined the relative expression levels of rat *Cyp1a2*, *Cyp2c11*,

and *Cyp2d2* in the liver of WT, Cyp3a-KO, and CYP3A-MAC/Cyp3a-KO rats (SI Appendix, Fig. S14). Cyp3a KO moderately increased the rat *Cyp1a2* expression level, while the expression level in CYP3A-MAC/Cyp3a-KO rats was similar to that in WT rats. The expression levels of rat *Cyp2c11* were highly increased in both Cyp3a-KO and CYP3A-MAC/Cyp3a-KO rats at a similar level. The rat *Cyp2d2* expression was moderately increased in both Cyp3a-KO and CYP3A-MAC/Cyp3a-KO rats. Thus, Cyp3a KO may affect the expression of other endogenous rat Cyp enzymes. On the other hand, since the hydroxylation activities of triazolam were much lower in the liver of Cyp3a-KO rats (Fig. 3D), Cyp enzymes increased by Cyp3a KO do not affect the metabolism of triazolam in the following functional study in CYP3A-humanized rats.

#### Functional Analyses in UGT2- and CYP3A-Humanized Rats.

**UGT2-humanized rats.** To analyze the function of human UGT2 in rats, zidovudine and gemfibrozil glucuronidation was investigated in WT, Ugt2-KO, and UGT2-MAC/Ugt2-KO rats. In the present study, these two medications were selected as UGT2-selective substrates. Zidovudine is mainly metabolized by human UGT2B7, which is an important isoform in UGT2 family (44). In the Ugt2-KO rats, no zidovudine glucuronidation activity was observed in the liver microsomes, indicating that rat Ugt2 is not functional in the liver. In contrast, higher zidovudine glucuronidation activity was observed in an incubation time-dependent manner in the liver microsomes that were prepared from UGT2-MAC/Ugt2-KO rats as well as those from WT rats and human



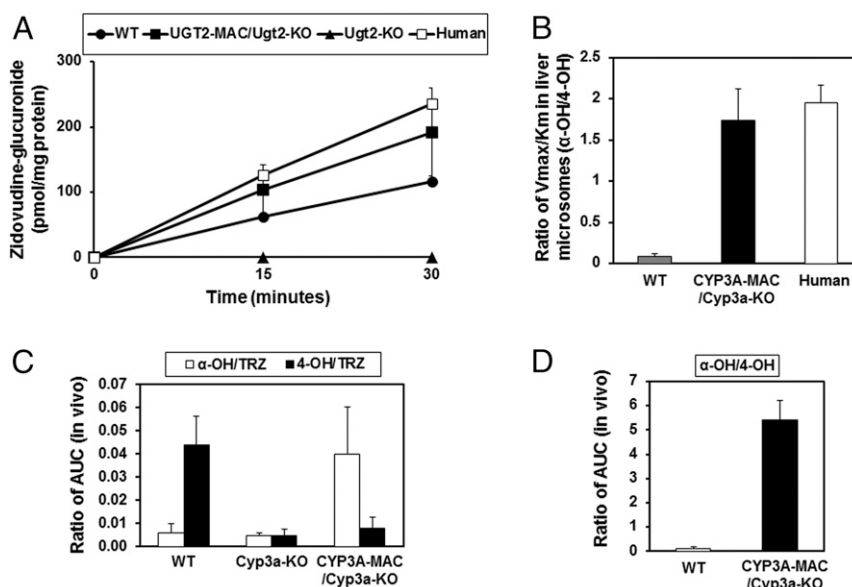


**Fig. 5.** Functional analyses of UGT2 and CYP3A in the liver of UGT2- and CYP3A-humanized rats. (A) Time-dependent change in the concentration of zidovudine glucuronide in the liver microsomes of WT rats, Ugt2-KO rats, UGT2-MAC/Ugt2-KO rats ( $n = 3$  for each group), and humans. (B) Ratios of intrinsic clearance ( $V_{max}/K_m$ ) for  $\alpha$ -OH triazolam (TRZ) and 4-OH TRZ formation in liver microsomes from WT rats (gray column), CYP3A-MAC/Cyp3a-KO rats (closed column), and humans (open column). Liver microsomes were prepared from PCN-treated WT and CYP3A-MAC/Cyp3a-KO rats. Kinetic parameters ( $V_{max}$  and  $K_m$ ) were determined as described in *Materials and Methods*. (C) Ratio of AUC for  $\alpha$ -OH TRZ/TRZ and 4-OH TRZ/TRZ in vehicle-treated WT, vehicle-Cyp3a-KO, and PCN-treated CYP3A-MAC/Cyp3a-KO rats. (D) Ratio of AUC for  $\alpha$ -OH TRZ/4-OH TRZ in vehicle-treated WT and PCN-treated CYP3A-MAC/Cyp3a-KO rats. Rats ( $n = 3$  for each group) were i.v. administered triazolam (2.5 mg/kg) through the tail vein. Data are derived from *SI Appendix, Table S3*.

triazolam and 4-OH triazolam between rats and humans, where the CYP3A-MAC/Cyp3a-KO rats more faithfully reflect the human situation than WT rats. Among the pharmacokinetic parameters calculated, clearances after i.v. and oral administration in Cyp3a-KO rats were lower than those in WT rats. Oral bio-availabilities in all strains were decreased by PCN treatment (*SI Appendix, Table S5*).

To further validate the value of the CYP3A-MAC/Cyp3a-KO rats for predicting human drug metabolism, we used midazolam, another common CYP3A probe drug. As shown in *SI Appendix, Fig. S21*, midazolam was preferentially metabolized to 4-OH midazolam in liver microsomes of WT rats. In contrast, 1'-OH midazolam was preferentially formed in liver microsomes of CYP3A-MAC/Cyp3a-KO rats and humans. In summary, our results show that CYP3A-MAC/Cyp3a-KO rats reflected the human metabolism of midazolam as well as triazolam. Taken together, these results strongly support the utility of CYP3A-MAC/Cyp3a-KO rats as a model to predict human drug metabolism.

## Discussion

In this study, we established a sophisticated strategy for the development of Mb-sized gene cluster humanized rat models by the approach of combining MMGT and genome editing technologies. We successfully cloned human Mb-sized gene clusters into MACs by a combination of telomere-directed chromosome truncation and loxP insertion in DT40 cells and Cre/loxP-mediated reciprocal translocation cloning in CHO cells. We subsequently introduced the MACs with Mb-sized human gene clusters into germline-competent rat ES cells. We demonstrated that MACs containing Mb-sized human gene clusters can be faithfully transmitted through the germline and maintained stably in rat tissues. Although the human *CYP3A* cluster had been previously cloned into HAC, the CYP3A-HAC was not mitotically stable in proliferative mouse tissues, such as spleen and bone marrow (16). In contrast, the CYP3A-MAC developed in this study were mitotically stable not only in mouse but also in rat tissues including organs with rapidly proliferating cells. Previously,

we showed that MACs were also stably maintained in human cell lines in vitro during long-term culture (19). Thus, MACs may be useful as common vectors for the generation of larger humanized animals such as pigs, cattle, and monkeys.

To the best of our knowledge, the maximal reported size of deletion in fertilized eggs via genome editing in rat for which germline transmission can still occur was 121.7 kb (47). In this study, we succeeded in generating a Ugt2 cluster KO rat line with a  $\sim 762$ -kb deletion. Previous endeavors to delete entire gene clusters mainly relied on labor- and time-intensive approaches using the Cre/loxP system, involving the targeting of two independent loxP sites at each end of the cluster, followed by Cre-mediated chromosomal deletion in ES cells and testing the capability of the ES cells to transmit the germline to the next generation at each step. Although such complex manipulations have been performed in mice, they are very difficult in rats owing to the chromosomal instability of rat ES cells. Therefore, the success of the large deletion in fertilized rat eggs described in this study is an important achievement and a prerequisite for the generation of fully humanized rats.

Rats are widely used for in vivo pharmacokinetic and drug-drug interaction studies for various reasons (48). Although rats are often considered as more advantageous models than mice for pharmacological study, the absence of complex genetic manipulation technologies in rat ES cells has thus far hindered the efficient generation of valuable humanized model rats. At least, the generation of Cyp-KO rats by genome editing have previously been described (49, 50). By combining the MAC approach with state-of-the-art genome engineering technologies, namely, TALEN and CRISPR/Cas9, the present study provides the successful generation of humanized UGT2 and CYP3A rats.

In this study, the tissue-specific expression pattern of *UGT2* and *CYP3A* genes observed in humans was reproduced in the humanized UGT2 and CYP3A rats. It should be noted that tissue-specific expression of *UGT2* and *CYP3A* genes has also been reported in the human prostate (41, 51). The analysis of the expression of UGT2 and CYP3A in prostate and their association

with cancer development using the humanized UGT2 and CYP3A rats will be an interesting subject for future investigations (52–54).

The conventional Tg methods using plasmids or BACs can be associated with altered gene expression due to position effects at the site of integration into the host genome and varying copy numbers of the transgenes, making faithful reproduction of human gene expression by this approach in different species very challenging. Since the MAC technology overcomes these limitations and a single MAC containing the genes of interest can be transferred readily to different species, the MAC approach has potential to provide a very powerful tool for achieving reproducible human gene expression in a variety of different species.

The analysis of species differences is an important application for rat models humanized for drug-metabolizing enzymes, such as those described in our study. Such species differences between humans and rats have been described for hepatic glucuronidation of gemfibrozil (55). Consistent with the previous finding, the glucuronidation rate of gemfibrozil was much lower in human than in rat liver microsomes (*SI Appendix, Fig. S15*). Notably, our humanized UGT2 rats also showed a lower rate of gemfibrozil glucuronidation than the wild-type rats (*SI Appendix, Fig. S15*), indicating that humanized rats can mimic human glucuronidation of this compound. It has also been reported that the rates of zidovudine glucuronidation are very similar between human and rat liver microsomes (56, 57) and the rates of zidovudine glucuronidation were also similar in liver microsomes prepared from our humanized UGT2 rats, wild-type rats, and human in our study (Fig. 5A). It therefore appears likely that the described humanized UGT rats are a useful tool to predict human drug glucuronidation.

In the present functional analyses of Cyp3a-KO and humanized CYP3A rats, we used triazolam as a probe drug. Triazolam is a highly specific CYP3A substrate and its clearance occurs almost entirely by hepatic metabolism by CYP3A after i.v. administration (58). First, in vitro studies showed that the formation rates of 4-OH triazolam in the liver microsomes of Cyp3a-KO rats were lower than those of WT rats (*SI Appendix, Fig. S16*). The in vitro findings were consistent with the in vivo findings that plasma concentrations of 4-OH triazolam in vehicle-treated Cyp3a-KO rats were lower than those in vehicle-treated WT rats (*SI Appendix, Fig. S19*). These results suggested that triazolam was preferentially metabolized to 4-OH triazolam by rat CYP3A enzymes in WT rats. Next, in vitro studies showed low formation rates of  $\alpha$ -OH triazolam and 4-OH triazolam in liver microsomes of vehicle-treated CYP3A-MAC/Cyp3a-KO and Cyp3a-KO rats (*SI Appendix, Fig. S16*). Plasma concentration profiles of  $\alpha$ -OH triazolam and 4-OH triazolam were also similar between vehicle-treated CYP3A-MAC/Cyp3a-KO and vehicle-treated Cyp3a-KO rats (*SI Appendix, Fig. S19*), suggesting that human CYP3A-dependent formation of  $\alpha$ -OH triazolam and 4-OH triazolam in vehicle-treated CYP3A-MAC/Cyp3a-KO rats was as low as in Cyp3a-KO rats. Importantly, however, PCN treatment increased the plasma concentrations of  $\alpha$ -OH triazolam over those of 4-OH triazolam in CYP3A-MAC/Cyp3a-KO rats, but not in Cyp3a-KO rats. These results suggested that the human CYP3A-dependent formation of  $\alpha$ -OH triazolam was enhanced by PCN treatment. Interestingly, plasma concentrations of 4-OH triazolam were markedly decreased and those of  $\alpha$ ,4-dihydroxytriazolam were largely increased by PCN only in WT rats (*SI Appendix, Figs. S19 A and D and S20*), suggesting that further metabolism of 4-OH triazolam to  $\alpha$ ,4-dihydroxytriazolam may be enhanced by PCN in WT rats. The further metabolism of 4-OH triazolam complicates the comparison of the AUC ratio of  $\alpha$ -OH triazolam and 4-OH triazolam between PCN-treated CYP3A-MAC/Cyp3a-KO and PCN-treated WT rats. Thus, the comparison of the AUC ratios in PCN-treated CYP3A-MAC/Cyp3a-KO rats with those in vehicle-treated WT rats appeared more accurate and was therefore undertaken in our analysis (Fig. 5D). Taking together the

findings of the in vitro (Fig. 5B) and in vivo studies (Fig. 5C and D), we observed that 4-OH triazolam preferentially formed in WT rats, but that  $\alpha$ -OH triazolam was mainly formed in CYP3A-MAC/Cyp3a-KO rats and humans.

Importantly, in these so-called humanized CYP3A and UGT2 rat strains, the pharmacokinetic profiles and metabolism of relevant probe substrates observed in humans were well reproduced. In this study, we used triazolam as a probe drug to compare the performance of CYP3A enzymes in humans and rats. However, the metabolism of not only triazolam but also midazolam showed different characteristics between humans and rats (59). The preferential formation of 1'-OH midazolam rather than 4-OH midazolam occurs in human liver microsomes. In contrast, midazolam is predominantly metabolized to 4-OH midazolam in rat liver microsomes. This feature found in human liver microsomes was found in CYP3A-MAC/Cyp3a-KO rats (*SI Appendix, Fig. S21*). Another difference between humans and rodents is the fact that CYP3A4 is expressed in human intestine and liver, whereas different CYP3A enzymes are expressed in both tissues in rodents (60). Owing to the human-like expression of CYP3A4 in liver and intestine of the described humanized rat, this model can also be applied to study differences of drug metabolism between humans and rodents resulting from the distinct tissue distribution of corresponding enzymes. Therefore, these humanized rats provide useful models not only for elucidating the mechanism of the temporal and spatial regulation of UGT2/CYP3A gene expression, but also for the improved prediction of human pharmacokinetics and drug–drug interactions.

Recently, we successfully modified the CYP3A5 single-nucleotide polymorphism (SNP) in the humanized CYP3A mouse using genome editing technology (61). The SNP conversion of CYP3A5 (g.6986G to A, \*3 to \*1) in the mouse ES cells and fertilized eggs recapitulated the CYP3A5\*1 carrier phenotype in humans. This SNP conversion method can also be applied to rat ES cells or rat fertilized eggs containing MACs with human genes, such as CYP3A- and UGT2-MACs, providing a means to readily establish relevant allelic human variants from an existing MAC humanized rat model. Thus, our approaches may be applicable to understand pharmacogenetic differences between major sequences and the variants in humans.

Whereas the UGT2/CYP3A models described in the present report have primary applications in drug metabolism and pharmacokinetic studies, it should be noted that the approach described herein has compelling utility for other applications. Since MACs can carry multiple and/or very large genes, and can be transmitted through the germline and stably maintained in vivo, this technology can be used to generate rat (and presumably other animal) models containing large genomic regions of genes with known species specificities, such as genes encoding other drug-metabolizing enzymes [CYP2C cluster (~400 kb)], drug transporters [OATP1 cluster (700 kb)], or components of the immune system [e.g., the HLA cluster (3 Mb), TCR $\alpha\delta$  (1 Mb), TCR $\beta$  (620 kb), IgH (~1.5 Mb), Igk (~2 Mb), and Igl (~1 Mb)].

In summary, the described combination of chromosome transfer of Mb-sized human gene clusters via MAC and genome editing for orthologous gene disruption provides a powerful approach for the generation of fully humanized Tc rats with various important applications in basic research, drug discovery, and development.

## Materials and Methods

**Cell Culture.** UGT2-MAC and CYP3A-MAC were constructed using a previously described Mb-sized gene cloning system via HAC (17, 31, 32). MAC4 and MAC1 vectors were used to generate the UGT2-MAC and CYP3A-MAC, respectively. The structure of MAC4 contained a centromere from mouse chromosome 11, EGFP flanked by HS4 insulators, 5'HPRT-loxP site, PGK-hyg, PGK-puro, and telomeres. The structure of MAC1 contained a centromere from mouse chromosome 11, EGFP flanked by HS4 insulators, PGK-neo, loxP-3'

HPRT site, PGK-puro, and telomeres (18). Chicken DT40 cells containing hChr.4 or hChr.7 were maintained at 40 °C in RPMI medium 1640 supplemented with 10% fetal bovine serum (FBS), 1% chicken serum, 50  $\mu$ M 2-mercaptoethanol, and 1.5 mg/mL G418 (62). Hprt-deficient CHO (hprt<sup>-/-</sup>) cells containing MAC4 or MAC1 used as fusion recipients for hChr.4 or hChr.7 transfer, respectively, were maintained at 37 °C in Ham's F-12 nutrient mixture (Invitrogen) supplemented with 10% FBS. Mouse embryonic fibroblasts (MEFs) were isolated from embryos at 13.5 day postcoitum (d.p.c.). MEFs were grown in DMEM (Sigma-Aldrich) plus 10% FBS. Parental mouse ES cell lines, TT2F, and the microcell hybrid TT2F clones were maintained on mitomycin C (Sigma-Aldrich)-treated Jcl:ICR (CLEA Japan) MEFs and neomycin-resistant MEFs (Oriental Yeast Co., Ltd.), respectively, as feeder layers in DMEM with 18% FBS (HyClone), 1 mM sodium pyruvate (Invitrogen), 0.1 mM nonessential amino acids (Invitrogen), 0.1 mM 2-mercaptoethanol (Sigma-Aldrich), 2 mM L-glutamine (Invitrogen), and 1,000 units/mL leukemia inhibitory factor (Funakoshi). A parental rat ES cell line (BLK2i-1, RGD ID: 10054010) and the microcell hybrid BLK2i-1 clones were maintained on mitomycin C-treated MEFs and neomycin-resistant MEFs, respectively, as feeder layers, as described previously (63).

**Modification of hChr.4 and hChr.7 in DT40 Cells.** Homologous recombination-proficient chicken DT40 cells ( $1 \times 10^7$ ) were collected in 0.5 mL of RPMI with 25  $\mu$ g of linearized targeting vector and electroporated at 550 V and 25  $\mu$ F using a Gene Pulser apparatus (Bio-Rad). Drug-resistant DT40 clones were selected in 1.5 mg/mL G418, 0.3  $\mu$ g/mL puromycin, 1.5 mg/mL hygromycin, or 0.5 mg/mL L-histidinol. Homologous recombination in DT40 hybrid clones was identified by PCR analyses using primers described in *SI Appendix, Table S1*.

**MMCT.** MMCT was performed as described previously (12). DT40 cells containing the modified chromosomes (hChr.4- $\Delta$ AC125239-loxP and hChr.7-loxP- $\Delta$ AC073842) were transferred to CHO (MAC4) and CHO (MAC1) cells, respectively, via MMCT. To transfer the UGT2-MAC or CYP3A-MAC to mouse ES cells and rat ES cells, CHO cells containing the UGT2-MAC or CYP3A-MAC were used as donor microcell hybrids. Briefly, mouse ES and rat ES cells were fused with microcells prepared from the donor hybrid cells, and selected with G418 (250 and 150  $\mu$ g/mL, respectively). The transferred UGT2-MAC and CYP3A-MAC in each line were characterized by PCR and FISH analyses.

**FISH Analyses.** The trypsinized cells and homogenized tissue samples were incubated for 15 min in 0.075 M KCl, fixed with methanol and acetic acid (3:1), and then slides were prepared using standard methods. FISH analyses were performed using fixed metaphase or interphase spreads of each cell hybrid

using digoxigenin-labeled (Roche) DNA [human COT-1 DNA/mouse COT-1 DNA (Invitrogen)] and biotin-labeled DNA [UGT2-BAC (RP11-643N16), CYP3A-BAC (RP11-757A13), mouse COT-1 DNA, PGK-neo,  $\beta$ -actin-hisD, PGK-puro, and PGK-hygro], essentially as described previously (12). Chromosomal DNA was counterstained with DAPI (Sigma-Aldrich). Images were captured using an AxioImagerZ2 fluorescence microscope (Carl Zeiss).

**Chimeric Rat Production.** Chimeric rats were produced as reported previously (64). Briefly, ES cells derived from each of the BLK2i-1 (UGT2-MAC) (nos. 1 and 2) and BLK2i-1 (CYP3A-MAC) (nos. 4, 8, 11, and 21) cell lines were microinjected into the blastocoel cavity of Crlj:WI E4.5 blastocysts (9–11 ES cells per blastocyst). Then, the blastocysts were transferred into uteri of pseudopregnant recipient rats at 3.5 d.p.c. (12–15 blastocysts per recipient). The contribution of the ES cells in the resultant offspring was confirmed by their coat color and/or fluorescence due to GFP gene expression. All animal experiments were approved by the Animal Care and Use Committee of National Institute for Physiological Sciences and Tottori University.

**ACKNOWLEDGMENTS.** We thank Toko Kurosaki, Yukako Sumida, Hiromichi Kohno, Masami Morimura, Kei Yoshida, Eri Kaneda, Akiko Ashiba, Dr. Kazuomi Nakamura, Rina Ohnishi, Etsuya Ueno, Kei Hiramatsu, Dr. Yoshiteru Kai, Motoshi Kimura, Chie Ishihara, Kiyoko Kawakami, Chiga Igawa (Tottori University), and Yuki Yamasaki (Chiba University) for their technical assistance; Dr. Hiroyuki Kugoh, Dr. Masaharu Hiratsuka, Dr. Tetsuya Ohbayashi, Dr. Takahito Ohira (Tottori University), Dr. Robert H. Tukey (University of California, San Diego), and Dr. Kan Chiba (Chiba University) for critical discussions; and the Edanz Group ([www.edanzediting.com/ac](http://www.edanzediting.com/ac)) for editing a draft of this manuscript. This study was supported in part by the Planned Collaborative Project and the Cooperative Study Program of the National Institute for Physiological Sciences, Japan (Y.K.); the City Area Program (Basic Stage) and Regional Innovation Strategy Support Program from the Ministry of Education, Culture, Sports, Science and Technology of Japan (MEXT) (M. Oshimura); the Takeda Science Foundation (M. Oshimura and Y.K.); the 21st Century Center of Excellence program from the Japan Society for the Promotion of Science (JSPS) (M. Oshimura); the Mochida Memorial Foundation for Medical and Pharmaceutical Research (Y.K.); the Naito Foundation (Y.K.); the Regional Innovation Strategy Support Program from MEXT (Y.K. and M. Oshimura); the Funding Program for Next Generation World-Leading Researchers (NEXT Program) from the JSPS (Y.K.); the Basis for Supporting Innovative Drug Discovery and Life Science Research from the Japan Agency for Medical Research and Development (AMED) under Grant JP18am0301009 (to Y.K.); the Basic Science and Platform Technology Program for Innovative Biological Medicine from AMED under Grant JP18am0101124 (to Y.K.); and JSPS KAKENHI Grant JP15H04285 (to Y.K.). This research was partly performed at the Tottori Bio Frontier managed by Tottori prefecture.

- Devoy A, Bunton-Stasyshyn RK, Tybulewicz VL, Smith AJ, Fisher EM (2011) Genomically humanized mice: Technologies and promises. *Nat Rev Genet* 13:14–20.
- Scheer N, Snaith M, Wolf CR, Seibler J (2013) Generation and utility of genetically humanized mouse models. *Drug Discov Today* 18:1200–1211.
- Abbott A (2004) Laboratory animals: The renaissance rat. *Nature* 428:464–466.
- Jacob HJ, Kwitek AE (2002) Rat genetics: Attaching physiology and pharmacology to the genome. *Nat Rev Genet* 3:33–42.
- Tong C, Li P, Wu NL, Yan Y, Ying QL (2010) Production of p53 gene knockout rats by homologous recombination in embryonic stem cells. *Nature* 467:211–213.
- Costantini F, et al. (1989) Insertional mutations in transgenic mice. *Prog Nucleic Acid Res Mol Biol* 36:159–169.
- Palminter RD, Brinster RL (1986) Germ-line transformation of mice. *Annu Rev Genet* 20:465–499.
- Soriano P, Gridley T, Jaenisch R (1987) Retroviruses and insertional mutagenesis in mice: Proviral integration at the Mov 34 locus leads to early embryonic death. *Genes Dev* 1:366–375.
- Lee EC, et al. (2014) Complete humanization of the mouse immunoglobulin loci enables efficient therapeutic antibody discovery. *Nat Biotechnol* 32:356–363.
- Macdonald LE, et al. (2014) Precise and in situ genetic humanization of 6 Mb of mouse immunoglobulin genes. *Proc Natl Acad Sci USA* 111:5147–5152.
- Oshimura M, Uno N, Kazuki Y, Katoh M, Inoue T (2015) A pathway from chromosome transfer to engineering resulting in human and mouse artificial chromosomes for a variety of applications to bio-medical challenges. *Chromosome Res* 23:111–133.
- Tomizuka K, et al. (1997) Functional expression and germline transmission of a human chromosome fragment in chimeric mice. *Nat Genet* 16:133–143.
- Tomizuka K, et al. (2000) Double trans-chromosomal mice: Maintenance of two individual human chromosome fragments containing Ig heavy and kappa loci and expression of fully human antibodies. *Proc Natl Acad Sci USA* 97:722–727.
- Shinohara T, et al. (2001) Mice containing a human chromosome 21 model behavioral impairment and cardiac anomalies of Down's syndrome. *Hum Mol Genet* 10:1163–1175.
- Kazuki Y, et al. (2011) Refined human artificial chromosome vectors for gene therapy and animal transgenesis. *Gene Ther* 18:384–393.
- Kazuki Y, et al. (2013) Trans-chromosomal mice containing a human CYP3A cluster for prediction of xenobiotic metabolism in humans. *Hum Mol Genet* 22:578–592.
- Kuroiwa Y, et al. (2000) Manipulation of human minichromosomes to carry greater than megabase-sized chromosome inserts. *Nat Biotechnol* 18:1086–1090.
- Tagikuchi M, et al. (2014) A novel and stable mouse artificial chromosome vector. *ACS Synth Biol* 3:903–914.
- Kazuki K, et al. (2013) Highly stable maintenance of a mouse artificial chromosome in human cells and mice. *Biochem Biophys Res Commun* 442:44–50.
- Kim H, Kim JS (2014) A guide to genome engineering with programmable nucleases. *Nat Rev Genet* 15:321–334.
- Wang L, et al. (2015) Large genomic fragment deletion and functional gene cassette knock-in via Cas9 protein mediated genome editing in one-cell rodent embryos. *Sci Rep* 5:17517.
- Boroviak K, Doe B, Banerjee R, Yang F, Bradley A (2016) Chromosome engineering in zygotes with CRISPR/Cas9. *Genesis* 54:78–85.
- Kraft K, et al. (2015) Deletions, inversions, duplications: Engineering of structural variants using CRISPR/Cas in mice. *Cell Rep* 10:833–839.
- Zhang L, et al. (2015) Large genomic fragment deletions and insertions in mouse using CRISPR/Cas9. *PLoS One* 10:e0120396.
- Martignoni M, Groothuis GM, de Kanter R (2006) Species differences between mouse, rat, dog, monkey and human CYP-mediated drug metabolism, inhibition and induction. *Expert Opin Drug Metab Toxicol* 2:875–894.
- Mackenzie PI, et al. (2005) Nomenclature update for the mammalian UDP glycosyltransferase (UGT) gene superfamily. *Pharmacogenet Genomics* 15:677–685.
- Fujiwara R, Yoda E, Tukey RH (2018) Species differences in drug glucuronidation: Humanized UDP-glucuronosyltransferase 1 mice and their application for predicting drug glucuronidation and drug-induced toxicity in humans. *Drug Metab Pharmacokin* 33:9–16.
- Kokura K, et al. (2016) A kidney injury molecule-1 (Kim-1) gene reporter in a mouse artificial chromosome: The responsiveness to cisplatin toxicity in immortalized mouse kidney S3 cells. *J Gene Med* 18:273–281.
- Yasunaga M, Fujita Y, Saito R, Oshimura M, Nakajima Y (2017) Continuous long-term cytotoxicity monitoring in 3D spheroids of beetle luciferase-expressing hepatocytes by nondestructive bioluminescence measurement. *BMC Biotechnol* 17:54.

30. Satoh D, et al. (2017) Establishment of a novel hepatocyte model that expresses four cytochrome P450 genes stably via mammalian-derived artificial chromosome for pharmacokinetics and toxicity studies. *PLoS One* 12:e0187072.
31. Kazuki Y, Oshimura M (2011) Human artificial chromosomes for gene delivery and the development of animal models. *Mol Ther* 19:1591–1601.
32. Hoshiya H, et al. (2009) A highly stable and nonintegrated human artificial chromosome (HAC) containing the 2.4 Mb entire human dystrophin gene. *Mol Ther* 17:309–317.
33. Mano Y, Usui T, Kamimura H (2007) The UDP-glucuronosyltransferase 2B7 isozyme is responsible for gemfibrozil glucuronidation in the human liver. *Drug Metab Dispos* 35:2040–2044.
34. Mahnke A, et al. (1997) Expression and inducibility of cytochrome P450 3A9 (CYP3A9) and other members of the CYP3A subfamily in rat liver. *Arch Biochem Biophys* 337:62–68.
35. Matsubara T, et al. (2004) Isolation and characterization of a new major intestinal CYP3A form, CYP3A62, in the rat. *J Pharmacol Exp Ther* 309:1282–1290.
36. Mandlekar SV, et al. (2007) Development of an in vivo rat screen model to predict pharmacokinetic interactions of CYP3A4 substrates. *Xenobiotica* 37:923–942.
37. Kobayashi K, Urashima K, Shimada N, Chiba K (2002) Substrate specificity for rat cytochrome P450 (CYP) isoforms: Screening with cDNA-expressed systems of the rat. *Biochem Pharmacol* 63:889–896.
38. Aueviriyavit S, Kobayashi K, Chiba K (2010) Species differences in mechanism-based inactivation of CYP3A in humans, rats and mice. *Drug Metab Pharmacokinet* 25:93–100.
39. Court MH, et al. (2012) Quantitative distribution of mRNAs encoding the 19 human UDP-glucuronosyltransferase enzymes in 26 adult and 3 fetal tissues. *Xenobiotica* 42:266–277.
40. Shelby MK, Cherrington NJ, Vansell NR, Klaassen CD (2003) Tissue mRNA expression of the rat UDP-glucuronosyltransferase gene family. *Drug Metab Dispos* 31:326–333.
41. Nishimura M, Yaguti H, Yoshitsugu H, Naito S, Satoh T (2003) Tissue distribution of mRNA expression of human cytochrome P450 isoforms assessed by high-sensitivity real-time reverse transcription PCR. *Yakugaku Zasshi* 123:369–375.
42. Komori M, et al. (1990) Fetus-specific expression of a form of cytochrome P-450 in human livers. *Biochemistry* 29:4430–4433.
43. Caron E, Rioux N, Nicolas O, Lebel-Talbot H, Hamelin BA (2005) Quantification of the expression and inducibility of 12 rat cytochrome P450 isoforms by quantitative RT-PCR. *J Biochem Mol Toxicol* 19:368–378.
44. Barbier O, et al. (2000) 3'-azido-3'-deoxythymidine (AZT) is glucuronidated by human UDP-glucuronosyltransferase 2B7 (UGT2B7). *Drug Metab Dispos* 28:497–502.
45. van Waterschoot RA, et al. (2009) Inhibition and stimulation of intestinal and hepatic CYP3A activity: Studies in humanized CYP3A4 transgenic mice using triazolam. *Drug Metab Dispos* 37:2305–2313.
46. Eberts FS, Jr, Philopoulos Y, Reineke LM, Vliet RW (1981) Triazolam disposition. *Clin Pharmacol Ther* 29:81–93.
47. Birling MC, et al. (2017) Efficient and rapid generation of large genomic variants in rats and mice using CRISMERE. *Sci Rep* 7:43331.
48. Iannaccone PM, Jacob HJ (2009) Rats! *Dis Model Mech* 2:206–210.
49. Lu J, et al. (2017) CRISPR knockout rat cytochrome P450 3A1/2 model for advancing drug metabolism and pharmacokinetics research. *Sci Rep* 7:42922.
50. Wang X, et al. (2016) Characterization of novel cytochrome P450 2E1 knockout rat model generated by CRISPR/Cas9. *Biochem Pharmacol* 105:80–90.
51. Turgeon D, Carrier JS, Lévesque E, Hum DW, Bélanger A (2001) Relative enzymatic activity, protein stability, and tissue distribution of human steroid-metabolizing UGT2B subfamily members. *Endocrinology* 142:778–787.
52. Karypidis AH, Olsson M, Andersson SO, Rane A, Ekström L (2008) Deletion polymorphism of the UGT2B17 gene is associated with increased risk for prostate cancer and correlated to gene expression in the prostate. *Pharmacogenomics J* 8:147–151.
53. Fujimura T, et al. (2009) Expression of cytochrome P450 3A4 and its clinical significance in human prostate cancer. *Urology* 74:391–397.
54. Leskelä S, et al. (2007) Cytochrome P450 3A5 is highly expressed in normal prostate cells but absent in prostate cancer. *Endocr Relat Cancer* 14:645–654.
55. Di Marco A, D'Antoni M, Attacalite S, Carotenuto P, Laufer R (2005) Determination of drug glucuronidation and UDP-glucuronosyltransferase selectivity using a 96-well radiometric assay. *Drug Metab Dispos* 33:812–819.
56. Sim SM, Back DJ, Breckenridge AM (1991) The effect of various drugs on the glucuronidation of zidovudine (azidothymidine; AZT) by human liver microsomes. *Br J Clin Pharmacol* 32:17–21.
57. Mano Y, Usui T, Kamimura H (2007) Comparison of inhibition potentials of drugs against zidovudine glucuronidation in rat hepatocytes and liver microsomes. *Drug Metab Dispos* 35:602–606.
58. Nolting A, Abramowitz W (2000) Lack of interaction between citalopram and the CYP3A4 substrate triazolam. *Pharmacotherapy* 20:750–755.
59. Ghosal A, Satoh H, Thomas PE, Bush E, Moore D (1996) Inhibition and kinetics of cytochrome P4503A activity in microsomes from rat, human, and cDNA-expressed human cytochrome P450. *Drug Metab Dispos* 24:940–947.
60. Komura H, Iwaki M (2008) Species differences in in vitro and in vivo small intestinal metabolism of CYP3A substrates. *J Pharm Sci* 97:1775–1800.
61. Abe S, et al. (2017) Modification of single-nucleotide polymorphism in a fully humanized CYP3A mouse by genome editing technology. *Sci Rep* 7:15189.
62. Kazuki Y, et al. (2004) Human chromosome 21q22.2-qter carries a gene(s) responsible for downregulation of mlc2a and PEBP in Down syndrome model mice. *Biochem Biophys Res Commun* 317:491–499.
63. Hirabayashi M, et al. (2013) A retrospective analysis of germline competence in rat embryonic stem cell lines. *Transgenic Res* 22:411–416.
64. Kobayashi T, et al. (2010) Generation of rat pancreas in mouse by interspecific blastocyst injection of pluripotent stem cells. *Cell* 142:787–799.